CHEMIJA. 2009. Vol. 20. No. 4. P. 208–217

Structure, NMR spectra and cytotoxic effect of palladium(II) and platinum(II) complexes of glyoxylic acid oxime

Nicolay I. Dodoff[1]*,

Maria Kubiak[2],

Janina Kuduk-Jaworska[2],

Agnieszka Mastalarz[2],

Andrzej Kochel[2],

Vladimira Vassilieva[1],

Nikolay Vassilev[3],

Natasha Trendafilova[4],

Ivelina Georgieva[4],

Maria Lalia-Kantouri[5],

Margariata Apostolova[1]

[1] *Acad. R. Tsanev Institute of Molecular Biology, Bulgarian Academy of Sciences, Sofia, Bulgaria*

[2] *Faculty of Chemistry, University of Wrocław, Poland*

[3] *Institute of Organic Chemistry with Centre of Phytochemistry, Bulgarian Academy of Sciences, Sofia, Bulgaria*

[4] *Institute of General and Inorganic Chemistry, Bulgarian Academy of Sciences, Sofia, Bulgaria*

[5] *Department of Chemistry, Aristotle University of Thessaloniki, Greece*

The structure of the complex K[Pd(GAO)(HGAO)] (**1**), where H_2GAO = glyoxylic acid oxime, has been determined by X-ray diffraction analysis. Orthorhombic crystals (*Pbca*, a = 15.890(2), b = 12.522(4), c = 16.703(3) Å, Z = 8) consist of two non-equivalent anionic complex molecules. Each complex molecule contains one mono- and one di-deprotonated H_2GAO molecules coordinated to Pd(II) *via* the carboxylato oxygen and oxime nitrogen atoms, forming two *cis*-oriented five-membered planar chelate rings. The two ligand molecules are connected via intramolecular hydrogen bond of the N–O···H–O–N type. The structure obtained is very similar to that of the analogous complex K[Pt(GAO)(HGAO)] · 3/4H_2O (**2**), deposited earlier. Complexes **1** and **2** were characterized by ^1H, ^{13}C and ^{195}Pt NMR spectra in water solution. Complex **2** exhibits a moderate cytotoxic activity (IC_{50} = 62 ± 16 μmol/l) and apoptogenic effect against the human leukemic cell line K562. In comparison with cisplatin, the complex shows a lower level of necrosis in the same cells and a higher aqueous solubility.

Key words: Pd(II) and Pt(II) complexes, glyoxylic acid oxime, crystal structure, NMR spectra, cytotoxic activity

INTRODUCTION

2-(Hydroxyimino)carboxylic acids have a structural similarity with α-aminocarboxylic acids. They possess a pronounced coordinating ability to metal ions and form various chelate complexes [1, 2] of technological [3–5] and pharmacological [6] significance. The application of oximes, including 2-(hydroxyimino)carboxylic acids, in organic synthesis has been recently reviewed [7]. Glyoxylic acid oxime (H_2GAO, (hydroxyimino)acetic acid) is the simplest representative of 2-(hydroxyimino)carboxylic acids. In the last years, we have published several articles on the elec-

* Corresponding author. E-mail: dodoff@obzor.bio21.bas.bg

tronic structure, vibrational spectra and conformational behaviour of H_2GAO [8] and its light transition metal complexes [9].

Ten years ago we firstly described [10] Pd(II) and Pt(II) complexes of H_2GAO, and, based on a detailed analysis of their vibrational spectra, suggested for them a bis-chelate structure with monodeprotonated ligand: $[M(HGAO)_2]$. Later, K. Mereiter [11] has solved the structure of the Pt(II) complex by X-ray crystallography and found that it is actually an ionic complex containing both the mono- and di-deprotonated chelate ligand $K[Pt(GAO)(HGAO)] \cdot 3/4H_2O$ (Fig. 1). We also confirmed the X-ray structural results of Mereiter. The mentioned complexes bear some resemblance (*cis*-oriented nitrogen and carboxylato-ligands) to the second-generation platinum anticancer drug, carboplatin (*cis*-diammine(1,1-cyclobutanedicarboxylato)platinum(II)) [12], and they are of interest as potential cytostatic agents. In the last years, Pt(II) complexes with imine N-donor atoms, like iminoethers [13, 14] and oximes [15], attract considerable attention in connection with the design of cytostatically active Pt(II) complexes with *trans*-configuration. Cu(II) complexes with oxime ligands have shown a cytostatic effect [16] and DNA cleavage activity [17–20]. At the same time, numerous oximes [21–23] and oxime ethers [24, 25] exhibit carcinostatic properties in a non-coordinated state. It should be emphasized that the Pt(II) and Pd(II) complexes of H_2GAO synthesized by us [10] have a good solubility in water. From the pharmacological point of view, this is an important property, taking into account that much efforts have been made to design platinum-based anticancer drugs with improved aqueous solubility compared to the parent compound, cisplatin (*cis*-$[Pt(NH_3)_2Cl_2]$) [12, 15, 26]. Although less explored and for the present having no clinical application, Pd(II) complexes with potential antitumor activity rouse increasing interest, as seen from a recently published review [27].

The present communication is a continuation and correction of our earlier work [10]. Here we report the X-ray crystallographic structure of the complex K[Pd(GAO)(HGAO)], NMR spectroscopic data and results from cytotoxic activity assays for the free ligand H_2GAO and its complexes K[Pd(GAO)(HGAO)] (**1**) and $K[Pt(GAO)(HGAO)] \cdot 3/4H_2O$ (**2**) (Fig. 1).

EXPERIMENTAL

Starting materials

K_2PdCl_4, K_2PtCl_4, glyoxylic acid monohydrate, hydroxylamine hydrochloride, and the remaining reagents and solvents were commercial products (*purum* or *pro analysi*). When necessary, the solvents were purified and distilled employing routine procedures. Cisplatin (*BioChemika*, 98%), MTT (3-(4,5-dimethy-2-thiazolyl)-2,5-diphenyl-2H-tetrazolium bromide) (*BioChemika*, ≥97.0%) and ethidium bromide (3,8-diamino-5-ethyl-6-phenylphenanthridinium bromide) (*BioChemika* for fluorescence, 98%) were from Fluka.

The ligand H_2GAO was prepared from glyoxylic acid monohydrate and hydroxylamine hydrochloride as described by Wieland [28], and recrystallized from ethylacetate – *n*-heptane; m. p. 139–140 °C.

Preparation of the complexes

The complexes were prepared as described earlier [10], with some modifications.

Potassium [{hydroxyimioacetato(1–)-*O*,*N*}{oxyiminoacetato(2–)-*O*,*N*}]palladate(II), K[Pd(GAO)(HGAO)] (1). 0.10 g (1.12 mmol) of H_2GAO was dissolved in water (1 ml), and the solution alkalized with aqueous K_2CO_3 to pH = 4. 0.18 g (0.55 mmol) of K_2PdCl_4 was dissolved in water (2 ml), the solution was filtered and the filter washed with a small volume of water (0.5 ml). The two solutions were mixed, shaken and left at room temperature in the dark for 48 h. The obtained yellow needle crystalline mass was filtered, washed with ethanol and dried *in vacuo*. Yield: 0.13 g (74%).

Potassium [{hydroxyimioacetato(1–)-*O*,*N*}{oxyiminoacetato(2–)-*O*,*N*}]platinate(II) hemisesquihydrate, K[Pt(GAO)(HGAO)] · 3/4H_2O (2). 0.09 g (1.01 mmol) of H_2GAO was dissolved in water (1.5 ml), and the solution was alkalized with aqueous K_2CO_3 to pH = 4. 0.21 g (0.51 mmol) K_2PtCl_4 was dissolved in water (1.2 ml), and the solution was filtered. Through the same filter the alkalized solution of H_2GAO was added, and finally the filter was washed with several drops of water. The reaction mixture was shaken and left at room temperature in the dark for 5 days. The red crystalline precipitate was filtered, washed with ethanol and dried *in vacuo*. Yield: 0.12 g (56%).

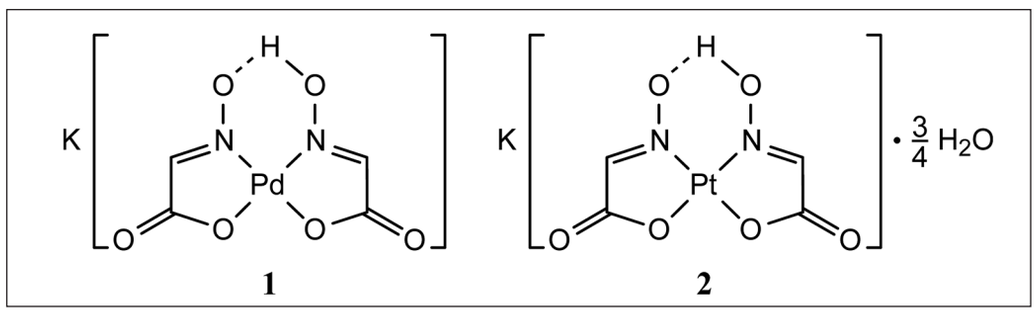

Fig. 1. Structural formulae of chelate complexes of glyoxylic acid oxime (H_2GAO): K[Pd(GAO)(HGAO)] (**1**) and $K[Pt(GAO)(HGAO)] \cdot (3/4)H_2O$ (**2**)

The complexes **1** and **2** were recrystallized from hot water. Well-shaped crystals suitable for X-ray diffraction analysis were obtained by dissolving *ca.* 30 mg of the corresponding complex in water (*ca*. 2 ml) in a short micro-tube upon slight heating. Then, the tube was covered with a stopper having a small hole, and the solution was left at room temperature in the dark until crystals appeared (*ca*. 10 days).

Caution! In solid state, complexes **1** and **2** are explosive. They detonate upon heating, and, probably, upon hitting. The complexes can be stored in normal conditions.

X-ray crystallography

The crystal of **1** was mounted on a glass fiber and flash-frozen to 100 K (Oxford Cryosystem-Cryostream Cooler). Preliminary examination and intensity data collection were carried out using a KM4-CCD diffractometer, ω scans, and graphite-monochromated Mo-Kα radiation generated from a diffraction X-ray tube operating at 50 kV and 20 mA. The data were corrected for Lorentz and polarization effects. Absorption corrections were performed for the intensity data (T_{min} = 0.710 and T_{max} = 0.873) [29]. The images were indexed, integrated, and scaled using the CrysAlis data reduction package [29]. The structure was solved by direct methods (SHELXS97) [30a] and refined by the full-matrix least-squares method on all F^2 data (SHELXL97) [30b]. The H(43o) and H(23o) atoms were included from difference Fourier map and refined isotropically, other H atoms were included from the geometry of molecules and were not refined. The N(21) and O(32) atoms are probably disordered, however, no satisfactory disorder model could have been proposed. Crystal data and details of data collection and refinement procedure are presented in Table 1.

Table 1. **Crystal data and structure refinement for 1***

Empirical formula	$C_8H_6K_2N_4O_{12}Pd_2$
M	641.17
T, K	100
λ, Å	0.71073
Crystal system	orthorhombic
Space group	*Pbca* (No 61)
a, Å	15.980(2)
b, Å	12.522(4)
c, Å	16.703(3)
V, Å^3	3323.5(13)
Z	8
D_{calcd}, g cm^{-3}	2.563
μ, mm^{-1}	2.740
F(000)	2464
Crystal colour, shape, size, mm	yellow, plates, 0.08 × 0.10 × 0.10
θ Range for data collection, deg	3.04–25.00
Limiting indices *h*, *k*, *l*	$-18 \le h \le 18$, $-8 \le k \le 14$, $-19 \le l \le 19$
Reflections collected	27186
Independent reflections	2923
R_{int}	0.1385
Data / parameters	2923 / 261
Goodness-of-fit (F^2)	1.025
Final R indices ($I > 2\sigma(I)$)	R_1 = 0.0456, wR_2 = 0.0606
R indices (all data)	R_1 = 0.0901, wR_2 = 0.0718
Largest diff. peak / hole, e Å^{-3}	1.052/–0.761

* CCDC 727197 contains the supplementary crystallographic data for this paper. These data can be obtained free of charge from the Cambridge Crystallographic Data Centre *via* www.ccdc.cam.ac.uk/data_request/cif.

NMR spectroscopy

NMR spectra of the compounds were recorded at 21–23 °C in D_2O (H_2GAO, **1** and **2**) and DMSO-d6 (H_2GAO only; TMS as internal standard) solutions. ^1H and ^{13}C NMR spectra were recorded on Bruker Avance 300 and Bruker Avance 500 spectrometers operating at 300.13 and 500.13, and 75.47 and 125.76 MHz for ^1H and ^{13}C spectra, respectively. The HOD signal (4.80 ppm) from the D_2O solvent, as well as the signals of acetone (one drop added to the samples dissolved in 0.5 ml of D_2O): $C\underline{H}_3$ (2.22 ppm), $^{13}\underline{C}H_3$ (30.89 ppm) and $^{13}\underline{C}$ = O (215.94 ppm) [31] were used as an internal standard for the ^1H and ^{13}C spectra. The ^{195}Pt NMR spectra were recorded on a Bruker Avance II+ 600 spectrometer at 129.01 MHz using BBO probehead. 1.2M Na_2PtCl_6 in D_2O (0.00 ppm) was used as external standard [32].

Cytotoxicity assays

Cell lines. Human leukemia cell line K562 (ATCC, CCL-243) and mouse leukemia cell line L1210 (ATCC, CCL-219) were cultured in DMEM (Dilbecco's Modified Eagle Medium, Applichem, Germany) supplemented with 10% (v/v) FBS (Fetal Bovine Serum, BioWhittaker, Cambrex Bio Science Verviers, Belgium), penicillin (100 μg/ml), streptomycin (100 μg/ml) and 4 mM L-glutamine (Biowhittaker, Boehringer Ingelheim, Germany) at 37 °C in a humidified atmosphere of 5% CO_2 and 95% air. Cells were routinely checked for mycoplasma contamination by DAPI staining (Roche Diagnostics, Mannheim, Germany) and found free of it.

Cell survival. All compounds (H_2GAO, **1**, **2**, cisplatin) were dissolved in sterile distilled water to obtain stock solutions which were then diluted with cell culture media to obtain the desired concentrations. For the drug sensitivity assay, cells were harvested and cultured for 24 h in a fresh medium, and were subsequently plated into 96-well microtitre plates (Nunc, Wiesbaden, Germany) at a density of $5 \cdot 10^4$ cells / well (100 μl). The sensitivity of the cell lines to different concentrations of the test compounds was determined at 24, 48, 72 and 96 h of drug exposure using the MTT assay of Mosmann [33]. The MTT-formazan product was dissolved in isopropanol, and the absorption at 550/630 nm was measured on an ELISA plate reader (Bio-Tek Instruments Inc., USA). The 50% inhibitory concentration (IC_{50}) is defined as the drug concentration needed to reduce population growth by 50%. The IC_{50} values were obtained by linear regression using Origin 6.0 software, and were received from eightplicates of MTT experiment.

DNA isolation and DNA fragmentation analysis. After 72 h of drug treatment, the cells were harvested and the standard protocol for DNA isolation was followed (Boehringer–Mannheim, Apoptotic DNA-ladder Kit). The cells were washed three times in phosphate-buffered saline (PBS) and collected by centrifugation at 5000 rpm for 5 min at 4 °C. The pellets were resuspended in 200 µl PBS and 200 µl binding buffer (6 M guanidine hydrochloride, 10 mM urea, 10 mM TRIS hydrochloride, 20% Triton X-100 (vol/vol), pH = 4.4) and incubated for 10 min at 72 °C. After incubation, 100 µl isopropanol was added for DNA precipitation. The DNA precipitates were carefully transferred to the filter tube, centrifuged at 8000 rpm for 1 min, and washed twice with a buffer containing 20 mM NaCl and 2 mM TRIS hydrochloride in ethanol (pH = 7.5). DNA was eluted from the filter with 200 µl pre-warmed (70 °C) 10 mM TRIS hydrochloride (pH = 8.5). DNA concentration was determined spectrophotometrically at 260 nm on a Beckman DU-650 spectrophotometer and considered pure when the ratio A_{260} / A_{280} (A_{260} and A_{280} are the absorptions at 260 and 280 nm, respectively) was between 1.6 and 2.0. The purified DNA (5 µg) was mixed with a loading buffer, and the samples were applied to 2.5% agarose gel (Seakem LE Agarose, Lonza) containing 5 µl/ml ethidium bromide. The electrophoresis was performed at 100 V in a vari-gel horizontal electrophoresis unit (Hofer Scientific Instruments, USA). The gel was visualized under UV light source and photographed.

Staining of apoptotic cells. The translocation of phosphatidylserine to the surface of apoptotic cells was determined with the Annexin V – fluorescein isothiocyanate (FITC) kit (Annexin V Apoptosis Detection Kit, SantaCruz, USA). After 72 h of drug treatment, cells were collected by low speed centrifugation at 1500 rpm for 5 minutes. The pellet was washed twice with cold PBS and resuspended in 1× Assay Buffer at a concentration of $1 \cdot 10^6$ cells/ml. Cell staining was achieved following the manufacturer's instruction (Annexin V Apoptosis Detection Kit, SantaCruz, USA) and immediately evaluated by fluorescence microscopy (AxioVert 200M, Zeiss, Germany). Approximately 1000 cells were count per each sample.

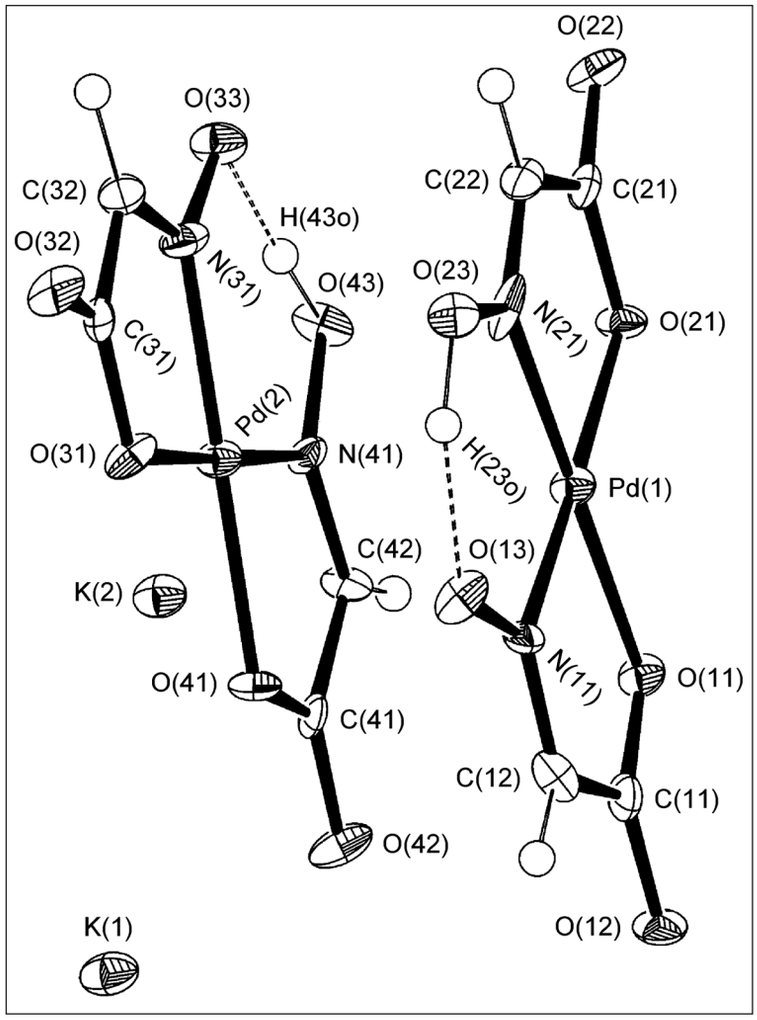

Fig. 2. ORTEP drawing for the molecular structure of K[Pd(GAO)(HGAO)] (**1**) with the atom labelling. Thermal ellipsoids are at 50% probability level

RESULTS AND DISCUSSION

Crystal structure of complex 1

Crystal structures of many similar compounds are described in the literature, e. g. the non-coordinated H_2GAO [8b, c, 34] and pyruvic acid oxime [35], as well as their chelate complexes with light transition metals [2c, d, 9b, 36a-e, 37], Ir(III) [36f], Zn(II) [9b, 38] and Cd(II) [9b]. The closest structural similarity exists, however, between the Pd(II) complex **1** and its Pt(II) analogue **2** [11]. These two structures are similar both at molecular and supramolecular levels, but, contrary to **2**, complex **1** does not contain water of hydration.

The single crystal X-ray diffraction analysis revealed that the structure of **1** involves two crystallographically non-equivalent anionic complex molecules and two independent potassium cations, as depicted in Fig. 2. Selected geometric parameters of the non-equivalent complex molecules are collected in Table 2. Each asymmetric monoanionic complex molecule includes one mono- and one di-deprotonated H_2GAO molecule coordinated to Pd(II) *via* the carboxylato oxygen and oxime nitrogen atoms. The two five-membered chelate rings with the common metal centre are condensed with a third six-membered ring with the participation of the intramolecular hydrogen bond between the deprotonated and non-deprotonated oxime groups. The geometry of the coordination node is very close to a planar tetragon of *cis*-PdN_2O_2 type. All the atoms in the complex anions are

Table 2. **Selected bond lengths, Å and angles, deg for 1**[a]

Bond lengths			
Pd(1)–N(11)	1.948(6)	Pd(2)–N(31)	1.959(6)
Pd(1)–N(21)	1.957(6)	Pd(2)–N(41)	1.958(6)
Pd(1)–O(11)	2.021(4)	Pd(2)–O(31)	2.011(5)
Pd(1)–O(21)	2.036(5)	Pd(2)–O(41)	2.032(5)
O(11)–C(11)	1.281(8)	O(31)–C(31)	1.308(9)
O(12)–C(11)	1.239(8)	O(32)–C(31)	1.216(9)
C(11)–C(12)	1.500(9)	C(31)–C(32)	1.508(11)
C(12)–N(11)	1.287(8)	C(32)–N(31)	1.288(9)
N(11)–O(13)	1.327(6)	N(31)–O(33)	1.336(7)
O(21)–C(21)	1.299(8)	O(41)–C(41)	1.294(8)
O(22)–C(21)	1.227(8)	O(42)–C(41)	1.232(8)
C(21)–C(22)	1.480(9)	C(41)–C(42)	1.486(9)
C(22)–N(21)	1.273(8)	C(42)–N(41)	1.279(8)
N(21)–O(23)	1.338(7)	N(41)–O(43)	1.333(7)
Pd(1)–Pd(2)	3.2096(14)	Pd(1)–Pd(2)^{i}	3.1566(14)
K(1)–O(32)^{iii}	2.608(5)	K(2)–O(42)^{iv}	2.636(5)
Bond angles			
N(11)–Pd(1)–O(11)	81.2(2)	N(31)–Pd(2)–O(31)	81.3(2)
O(11)–Pd(1)–O(21)	101.22(18)	O(31)–Pd(2)–O(41)	100.85(19)
N(21)–Pd(1)–O(21)	80.3(2)	N(41)–Pd(2)–O(41)	80.7(2)
N(11)–Pd(1)–N(21)	97.4(2)	N(31)–Pd(2)–N(41)	97.1(2)
Pd(2)^{i}–Pd(1)–Pd(2)	159.403(19)	Pd(1)^{ii}–Pd(2)–Pd(1)	176.53(2)
Torsion angles			
O(13)–N(11)–Pd(1)–N(21)	1.4(6)	O(33)–N(31)–Pd(2)–N(41)	1.1(6)
O(23)–N(21)–Pd(1)–N(11)	2.2(6)	O(43)–N(41)–Pd(2)–N(31)	–0.4(6)
N(31)^{i}–Pd(2)^{i}–Pd(1)–N(11)	125.6(3)	N(11)–Pd(1)–Pd(2)–N(31)	125.6(3)
N(31)–Pd(2)–Pd(1)^{ii}–N(11)^{ii}	–125.6(3)	Pd(2)^{i}–Pd(1)–Pd(2)–Pd(1)^{ii}	–160.2(4)
Dihedral angles between least-squares planes[b]			
ρ, σ	1.01(4)	τ,ν	2.57(5)

[a] Symmetry codes: ^{i} –x + 1/2, y + 1/2, z; ^{ii} –x + 1/2, y – 1/2, z; ^{iii} x – 1/2, y, –z – 1/2;
^{iv} x + 1/2, y, – z – 1/2; [b] Atoms used to define planes and RMS deviations (Å) of fitted atoms in parentheses: ρ, Pd(1)–O(11)–C(11)–C(12)–N(11) (0.0059); σ, Pd(1)–O(21)–C(21)–C(22)–N(21) (0.0104); τ, Pd(2)–O(31)–C(31)–C(32)–N(31) (0.0227); ν, Pd(2)–O(41)–C(41)–C(42)–N(41) (0.0091).

practically coplanar, as seen from the relevant torsion angles (typically about 1–3°), least squares planes and dihedral angles between them (less than 3°). The geometric parameters of the two independent complex anions are very similar; e. g., for the coordination node, the differences in the bond lengths are less than 0.025 Å, and in the bond angles less than 1°. The two intramolecular hydrogen bonds N–O···H–O–N (Table 3) have also a similar geometry, both of them forming quite obtuse angles O···H–O (168(7) and 173(12)°). At the molecular level, there is a qualitative as well as quantitative structural resemblance between complexes **1** and **2** [11]. Thus, in both cases there are two crystallographically non-equivalent, practically planar complex anions with the same mode of coordination and the same type of hydrogen bonding. The geometric parameters of **1** and **2** are quite similar (typically, the differences in the bond lengths are less than 0.04 Å, and in the bond angles about 1–2°). Cu(II) [2d, 36a], Co(III) [36d] and Ni(II) [36b] complexes of pyruvic acid oxime could be mentioned as other examples of 2-(hydroxyimino)carboxylic acid bis-chelate structures containing both deprotonated and non-deprotonated oxime groups. In crystalline state, the free H_2GAO forms hydrogen-bonded cyclic tetramers [8b, c, 34] like the free pyruvic acid oxime [35]. A comparison between the free H_2GAO and its complexes **1** and **2** shows that coordination of the ligand to Pd(II) and Pt(II) leads to a decrease in the bond lengths O–N and C–O and an increase in the bond lengths C = N, C = O and C–C.

The crystal packing for **1** is depicted in Fig. 3. The centrosymmetric unit cell contains eight pairs of complex anions together with the corresponding potassium cations. The almost planar complex molecules are ordered in *quasi*-parallel layers with respect to the crystallographic axes *a* and *c*. The distances between the corresponding ring centroids are summarized in Table 3. Along the *b* axis, the complex molecules are arranged one on the top of another being rotated at 125.6(3) and –125.6(3)° (see Table 2). The Pd(II) ions form a strongly flattened zig-zag line with Pd–Pd distances of 3.2096(14) and 3.1566(14) Å and a torsion angle of –160.2(4)° (Table 2). At the crystal packing level, the structural analogy between complexes **1** and **2** continues. Thus, although crystals of **1** belong to the orthorhombic system (space group *Pbca*) (Table 1) and **2** crystallizes in a monoclinic system (space group *C*2/*c*), the

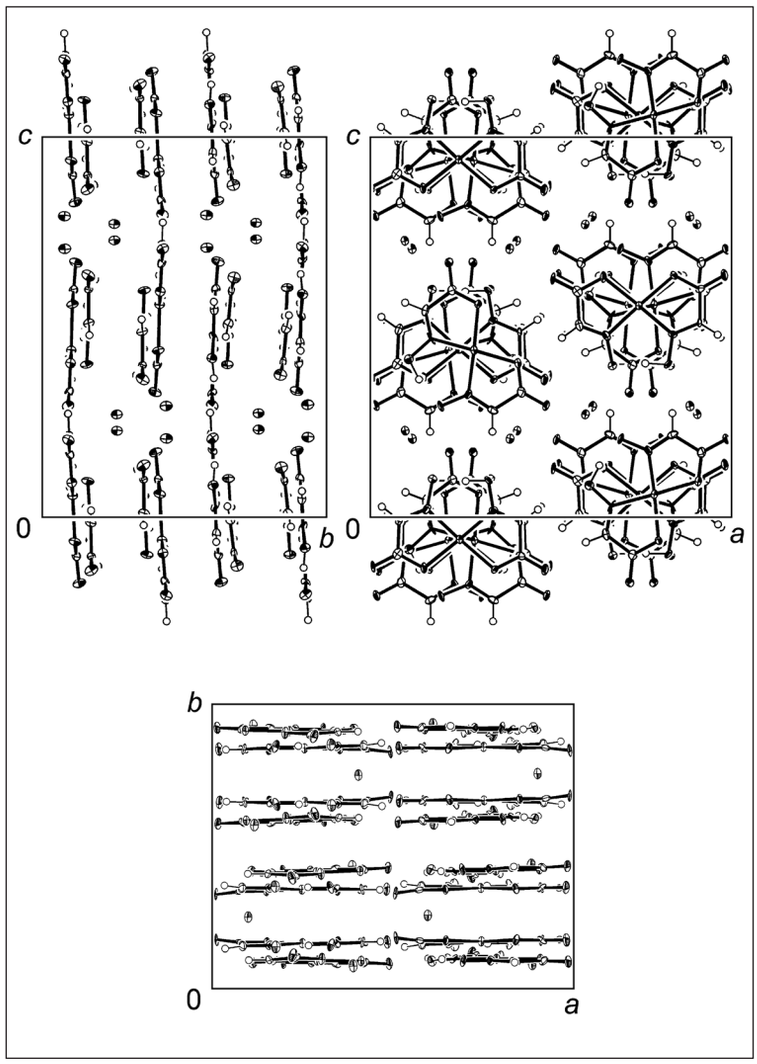

Fig. 3. View of the unit cell of K[Pd(GAO)(HGAO)] (**1**) along the axes *a*, *b* and *c*, respectively

unit cell lengths in the two cases are quite similar, and the cell angle β in **2** (91.13(1)°) is very close to the right angle. Like in **1**, the unit cell of **2** contains eight couples of molecules, which are again arranged one on the top of another. The distances Pt–Pt (3.2739(12) and 3.2109(10) Å [11]) are longer than the distances Pd–Pd in **1** (Table 2).

NMR spectra

The free ligand H_2GAO and its complexes **1** and **2** were characterized by ^{1}H, ^{13}C and ^{195}Pt NMR spectroscopy, and relevant data are summarized in Table 4.

In the ^{1}H NMR spectrum of H_2GAO taken in DMSO-d6, signals of all the three protons were detected, whereas for D_2O solutions only the signal of azomethine proton of the free ligand and of the complexes **1** and **2** can be observed. The signal appears as a singlet in the range of 7.33–7.72 ppm, which, in the case of **2**, has a satellite doublet signal due to the vicinal coupling with the ^{195}Pt nucleus (natural abundance *ca*. 34%) [39, 40]. The position of the signal is similar to that of the corresponding signal in ^{1}H NMR spectra of Zn(II) chelate of H_2GAO (7.50 ppm) [5], as well as of glyoxylic acid thiosemicarbazone and its Pt(II) complex (7.29 and 7.36 ppm, respectively) [42]. It is noteworthy that the $^{3}J(^{195}\text{Pt}-^{1}\text{H})$ constant for **2** is quite large – 80 Hz. It exceeds the corresponding constant for the Pt(II) complex of glyoxylic acid thiosemicarbazone (61 Hz) [42], as well as almost all of the values for $^{3}J(^{195}\text{Pt}-^{1}\text{H})$ constants

Table 3. **Geometry of hydrogen bonding, Å and degree, and distances between ring centroids, Å for 1**[a, b]

D–H···A		D–H	H···A	D···A	∠D–H···A
O(23)–H(23o)···O(13)		0.96(8)	1.55(8)	2.490(7)	168(7)
O(43)–H(43o)···O(33)		0.93(10)	1.53(10)	2.460(8)	173(12)
Cg1→Cg4	Cg2→Cg3	Cg1→Cg3[i]	Cg2→Cg4[i]	Cg3→Cg1[ii]	Cg4→Cg2[ii]
3.508(4)	3.626(4)	3.394(4)	3.662(4)	3.394(4)	3.662(4)

[a] Symmetry codes: [i] –x + 1/2, y + 1/2, z; [ii] –x + 1/2, y – 1/2, z;

[b] Cg1, Cg2, Cg3 and Cg4 refer to the centroids: Pd(1)–O(11)–C(11)–C(12)–N(11), Pd(1)–O(21)–C(21)–C(22)–N(21), Pd(2)–O(31)–C(31)–C(32)–N(31) and Pd(2)–O(41)–C(41)–C(42)–N(41), respectively.

Table 4. **^{1}H, ^{13}C and ^{195}Pt NMR spectroscopic data for H_2GAO and its complexes in D_2O solution**

Compound	Chemical shift (δ, ppm), multiplicity[a]				Coupling constant (*J*, Hz)		
	^{1}HC = N	H^{13}C = N	^{13}COO	^{195}Pt	$^{1}J(^{13}\text{C}-^{1}\text{H})$	$^{2}J(^{13}\text{C}-^{1}\text{H})$	$^{3}J(^{195}\text{Pt}-^{1}\text{H})$
H2GAO[b]	7.58 s + 2 d	144.0 d	167.0 d	–	176.6	8.8	–
1	7.33 s + 2 d	141.0 d	174.4 d	–	187.2	9.2	–
2	7.72 s + 3 d	137.7 d	177.5 d	–1919 s	190.5	9.3	80

[a] Notations. d: Doublet; s: singlet; s + 2 d: singlet with two ^{13}C satellites; s + 3 d: singlet with two ^{13}C satellites and one ^{195}Pt satellite.

[b] ^{1}H NMR data in DMSO-d_6 solution: δ, ppm ($J(^{13}\text{C} - ^{1}\text{H})$, Hz). HC = N: 7.44 1H s + 2 d (^{1}J = 172.5, ^{2}J = 8.5); NOH and COOH: 12.37 1H s, 13.00 1H s, broad.

collected by Rochon et al. in their review [40] and in newer papers [43]. Under appropriate expansion, two weak satellite signals originating from the coupling with ^{13}C nucleus [41] were observed. The first one comes from the one-bond coupling ($^1J(^{13}C–^1H)$ = 176.6–190.5 Hz), and the second is due to the geminal coupling ($^2J(^{13}C–^1H)$ = 8.8–9.3 Hz) and appears as shoulders around the main signal. The mentioned features of the ^1H spectra are illustrated in Fig. 4A on the example of complex **2**.

Signals in the ^{13}C NMR spectra of H_2GAO and complexes **1** and **2** (Table 4) appear in the expected ranges for azomethine and carboxylic carbon atoms [44,45]. The chemical shifts for the two types of carbons can be compared with those of the Zn(II) complex of H_2GAO (146 and 168 ppm, respectively) [5] and of glyoxylic acid thiosemicarbazone and its Pt(II) complex (142.3 and 174.6 ppm, respectively) [42]. The ^{13}C NMR spectrum of **2** is shown in Fig. 5. The values of the $^1J(^{13}C–^1H)$ and $^2J(^{13}C–^1H)$ coupling constants obtained from the ^{13}C NMR spectra confirm the assignment of ^{13}C satellite signals in the ^1H spectra (*cf.* Figs. 4A and 5). We failed to detect the $^2J(^{13}C–^{195}Pt)$ coupling constants, most probably because of the small values of such constants and of the effect of chemical shift anisotropy [40].

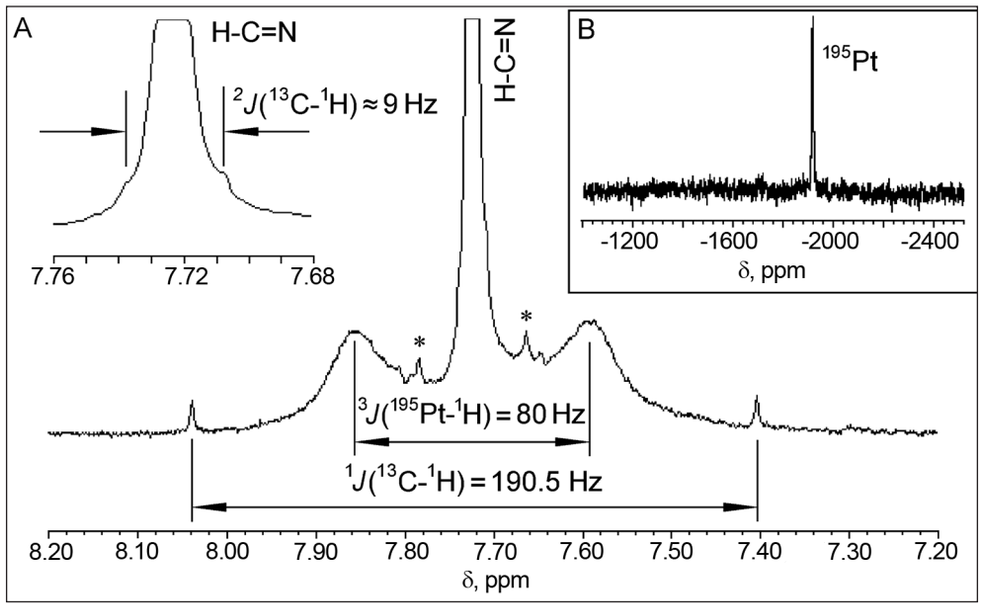

Fig. 4. NMR spectra of K[Pt(GAO)(HGAO)] · (3/4)H_2O (**2**) in D_2O with assignments. A) ^1H spectrum (expanded) showing ^{13}C and ^{195}Pt satellites of the HC = N signal. Spinning sidebands due to sample rotation [46] (18 Hz) are marked with asterisks. B) ^{195}Pt spectrum

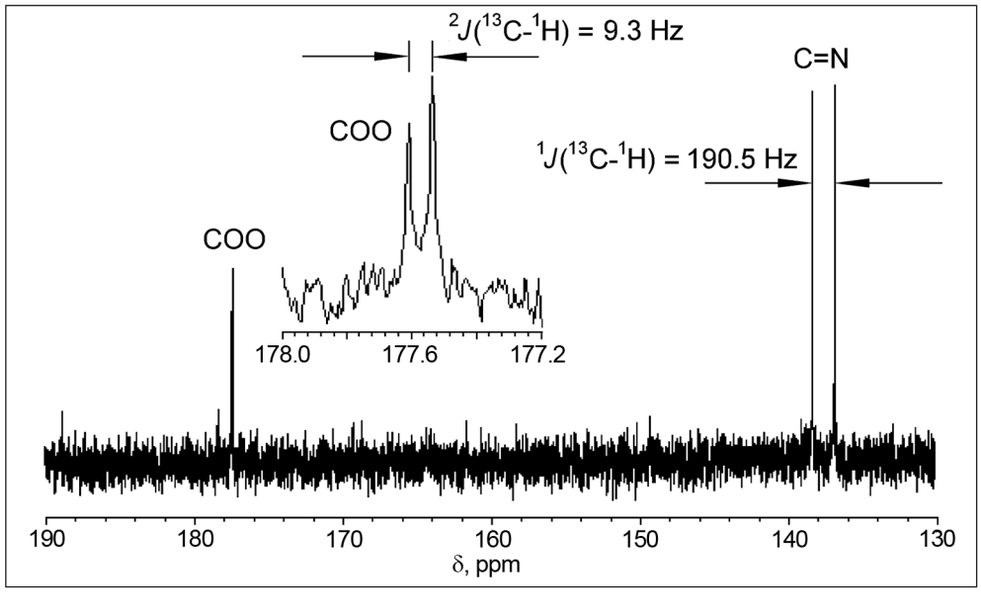

Fig. 5. ^{13}C NMR spectrum of K[Pt(GAO)(HGAO)] · (3/4)H_2O (**2**) in D_2O with assignments

Complex **2** gives a single ^{195}Pt resonance at –1919 ppm (Table 4, Fig. 4B). The value falls in the range typical of Pt(II) complexes with the PtN_2O_2 coordination node [39, 40]. It should be noted that in all NMR spectra of complexes **1** and **2**, only one set of signals is observed, which indicates the equivalence of the two ligand molecules in aqueous solution.

Cytotoxic effects

Cell growth inhibition. The cytotoxic effect of the ligand and its complexes, together with cisplatin as a positive control, was examined against mouse leukemia L1210 and human leukemia K562 cells. The results of cell survival assays at various drug concentrations, along with the calculated 50% inhibitory concentrations (IC_{50}), are presented in Fig. 6. H_2GAO and its Pd(II) complex **1** were inactive against the two cell lines (IC_{50} > 300 µmol/l). The Pt(II) complex **2** exhibited a pronounced effect against L1210 leukemia (17 ± 5% living cells) only at a concentration of 300 µmol/l. The IC_{50} value is, however, too high: 221 ± 18 µmol/l. Compared to cisplatin in our experiment and to data of Reedijk et al. [47] about carboplatin in the same cell line, this value appears *ca.* 44 and 22 times higher, respectively.

Against K562 cell line, complex **2** showed a moderate activity: IC_{50} = 62 ± 16 µmol/l. This value is roughly 60 times higher than the IC_{50} value of cisplatin in our test, and 8 times higher than that reported for carboplatin against the same human leukemia cell line [48]. At the same time, the aqueous solubility of complex **2** at a normal temperature (>59 mmol/l) is higher than that of cisplatin (*ca.* 8 mmol/l) [49] and carboplatin (*ca.* 40 mmol/l) [50].

Induction of apoptosis. In contrast to necrosis, apoptosis is the less drastic and physiologically normal way of cell death [51]. The induction of apoptosis is known to be a key process responsible for cisplatin cytotoxicity [52]. We applied two approaches for detecting apoptotic cells: the electrophoresis assay of DNA frgmantation (DNA laddering test) [51] and the technique for fluorescent detection of the Annexin V binding to membrane phospholipids combined with propidium iodide staining, which permits to distinguish between apoptotic and necrotic cells [51].

The results of DNA fragmentation assay are illustrated in Fig. 7. Genomic DNA isolated from K562 cells treated with complex **2** (35 µmol/l) showed a pattern of DNA ladder formation indicative of apoptosis, in contrast to the control and H_2GAO-treated cells. Compared with cisplatin as a reference, **2** showed a similar level of DNA fragmentation, whereas signs

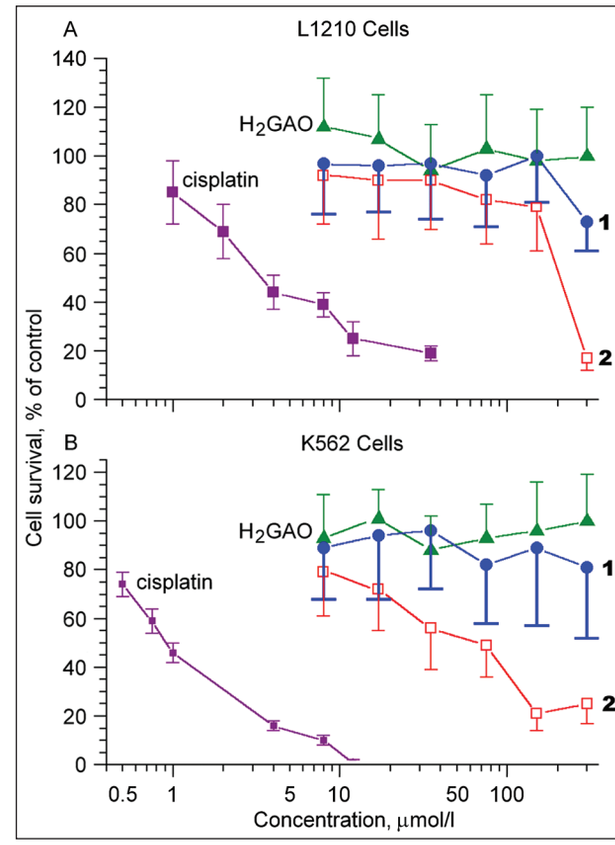

Fig. 6. Cytotoxic effect of different concentrations of cisplatin, H_2GAO and its complexes K[Pd(GAO)(HGAO)] (**1**) and K[Pt(GAO)(HGAO)] · (3/4)H_2O (**2**) against L1210 (A) and K562 (B) cells after 72 h of drug exposure. Values are mean of at least four independent experiments with standard deviations (SD). Inhibitory concentrations IC_{50} ± SD in µmol/l: L1210 cells – 5 ± 2 (cisplatin), >300 (H_2GAO and **1**), 221 ± 18 (**2**); K562 cells – 1.1 ± 0.5 (cisplatin), >300 (H_2GAO and **1**), 62 ± 16 (**2**)

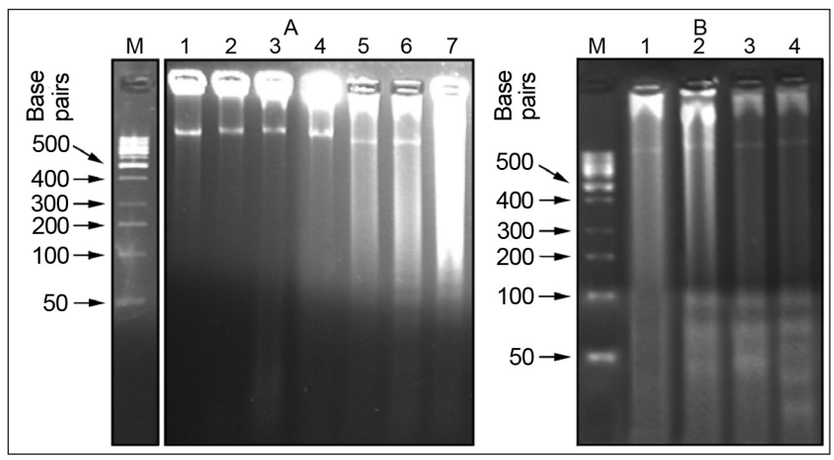

Fig. 7. Agarose gel electrophoresis of internucleosomal DNA of human leukemia K562 cells (A) and mouse leukemia L1210 cells (B) after 72 h of treatment with the test compounds. A: M – 1 kb DNA size marker; 1, 2 – control; 3, 4 – H_2GAO (35 µmol/l); 5, 6 – K[Pt(GAO)(HGAO)] · (3/4)H_2O (**2**) (35 µmol/l); 7 – cisplatin (0.75 µmol/l). B: M – 1kb DNA size marker; 1 – control; 2, 3 – **2** (150 µmol/l); 4 – cisplatin (2 µmol/l)

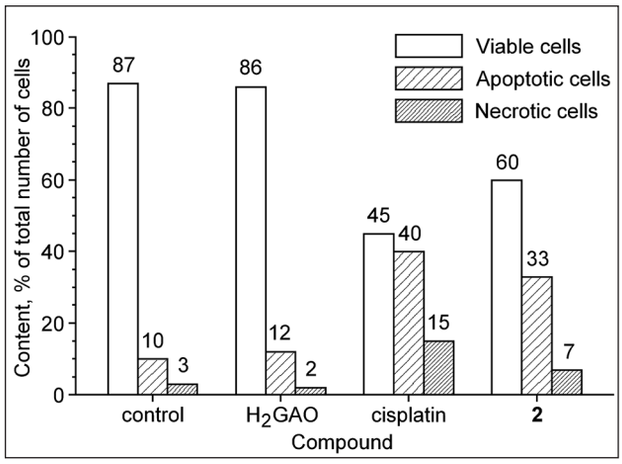

Fig. 8. Results of the Annexin V – fluorescein isothiocyanate quantification of apoptotic and necrotic cells in human leukemia K562 cells treated (72 h) with H_2GAO (35 μmol/l), cisplatin (0.75 μmol/l) and K[Pt(GAO)(HGAO)] · (3/4)H_2O (**2**) (35 μmol/l). The total number of cells counted to calculate the percentage of living, apoptotic and necrotic cells was 1040 (control), 936 (H_2GAO), 1405 (**2**) and 1030 (cisplatin)

of necrosis were less manifested (Fig. 7A). Against L1210 cells, complex **2** was much less cytotoxic, but DNA fragmentation was clearly observed at a drug concentration of 150 μmol/l (Fig. 7B).

To further confirm the results obtained by DNA fragmentation assay and to distinguish between apoptotic and necrotic cells, we performed the Annexin V – fluorescein isothiocyanate staining test for the K562 cell line, the results of which are summarized in Fig. 8. H_2GAO practically did not affect the percentage of apoptotic and necrotic cells with respect to the control. However, treatment with **2** caused an increase in the percentage of apoptotic and necrotic cells 3.3 and 2.3 times, respectively, as compared to the control. A comparison with cisplatin reveals that complex **2** is a softer cytotoxic agent, exhibiting a *ca*. two-fold weaker necrotic effect. Cisplatin showed a four- and five-fold increase in the content of apoptotic and necrotic cells, respectively, with respect to the control.

CONCLUSIONS

The structure of Pd(II) and Pt(II) complexes with the ligand H_2GAO, earlier described by us [10], was corrected on the basis of X-ray crystallography and NMR spectroscopy. The compounds are anionic bis-chelate complexes containing both mono- and di-deprotonated *N*,*O*-coordinated ligand molecules with an intramolecular hydrogen bond: K[Pd(GAO)(HGAO)] and K[Pt(GAO)(HGAO)] · 3/4H_2O. The Pt(II) complex exhibited a moderate cytotoxic activity (IC_{50} = 62 ± 16 μmol/l) and apoptogenic effect on human leukemic cells K562. Compared to cisplatin, the complex showed a lower level of necrosis against the same cell line and a better water solubility. Complexes of this type deserve further attention as potential cytostatic agents.

ACKNOWLEDGEMENTS

Thanks are due to Professor Kurt Mereiter for placing his unpublished data at our disposal and to Dr. Tzvetan Mihaylov for the preparation of the ligand H_2GAO. The work is part of the bilateral cooperation between the Bulgarian Academy of Sciences and the Aristotle University of Thessaloniki for the period 2009–2012, and has been supported by the Bulgarian National Research Fund (Project UNA-17/2005).

Received 27 July 2009
Accepted 17 August 2009

References

1. M. E. Keeney, K. Osseo-Asare, K. A. Woode, *Coord. Chem. Rev.*, **59**, 141 (1984).
2. a) T. Yu. Sliva, A. Dobosz, L. Jerzykiewicz, A. Karaczyn, A. M. Moreeuw, J. Świątek-Kozłowska, T. Głowiak, H. Kołzowski, *J. Chem. Soc., Dalton Trans.*, 1863 (1998); b) A. A. Mokhir, E. Gumienna-Kontecka, J. Świątek-Kozłowska, E. G. Petkova, I. O. Fritsky, L. Jerzykiewicz, A. A. Kapshuk, T. Yu. Sliva, *Inorg. Chim. Acta,* **329**, 113 (2002); c) A. Dobosz, N. M. Dudarenko, O. I. Fritsky, T. Głowiak, A. Karaszyn, H. Kołzowski, T. Yu. Sliva, J. Świątek-Kozłowska, *J. Chem. Soc., Dalton Trans.,* 743 (1999); d) K. Malek, M. Vala, J. Świątek-Kozłowska, L. M. Proniewicz, *New J. Chem.*, **28**, 477 (2004); e) K. Malek, H. Kołzowski, L. M. Proniewicz, *Polyhedron*, **24**, 1175 (2005).
3. A. W. Apblett, G. D. Georgieva, *Phosphorus, Sulfur, Silicon Relat. Elem.*, **93–94**, 479 (1994).
4. Z. Zhang, R. Liu, M. Zhao, Y. Qian, *Mater. Chem. Phys.*, **71**, 161 (2001).
5. M. R. Hill, A. W. Jones, J. J. Russell, N. K. Roberts, R. N. Lamb, *Inorg. Chim. Acta*, **358**, 201 (2005).
6. a) Yu. V. Shklyaev, B. Ya. Syropyatov, V. S. Shklyaev, M. S. Gavrilov, E. S. Boronenkova, R. Z. Dautova, B. B. Aleksandrov, A. A. Gorbunov, *Pharm. Chem. J.*, **33**, 467 (1999); b) V. O. Koz'minykh, E. N. Koz'minykh, *Pharm. Chem. J.*, **38**, 67 (2004).
7. A. I. Mikhaleva, A. B. Zaitsev, B. A. Trofimov, *Russian Chem. Rev.*, **75**, 797 (2006).
8. a) N. Trendafilova, G. Bauer, I. Georgieva, V. Delchev, *J. Mol. Struct.*, **604**, 211 (2002); b) I. Georgieva, D. Binev, N. Trendafilova, G. Bauer, *Chem. Physics*, **286**, 205 (2003); c) I. Georgieva, N. Trendafilova, D. Binev, *Vibr. Spectrosc.*, **31**, 143 (2003); d) I. Georgieva, N. Trendafilova, *Chem. Physics*, **321**, 311 (2006).
9. a) I. Georgieva, N. Trendafilova, L. Rodríguez-Santiago, M. Sodupe, *J. Phys. Chem.*, *A*, **109**, 5668 (2005); b) I. Georgieva, N. Trendafilova, G. Bauer, *Spectrochim. Acta*, *A*, **63**, 403 (2006).
10. N. Trendafilova, G. Bauer, I. Georgieva, N. Dodoff, *Spectrochim. Acta*, *A*, **55**, 2849 (1999).
11. K. Mereiter, Private Communication, CCDC-242816 (2004).
12. a) M. A. Jakupec, M. Galanski, B. K. Keppler, *Rev. Physiol. Biochem. Pharmacol.*, **146**, 1 (2003); b) M. Galanski, *Rec. Pat. Anti-Cancer Drug Discov.*, **1**, 285 (2006); c) I. Kostova, *Rec. Pat. Anti-Cancer Drug Discov.*, **1**, 1 (2006).

13. a) M. Coluccia, G. Natile, *Anti Cancer Agents Med. Chem.*, **7**, 111 (2007); b) U. Kalinowska-Lis, J. Ochocki, K. Matlawska-Wasowska, *Coord. Chem. Rev.*, **252**, 1328 (2008).
14. S. Mazzega Sbovata, F. Bettio, C. Marzano, A. Tassan, M. Mozzon, R. Bertani, F. Benetollo, R. A. Michelin, *J. Inorg. Biochem.*, **102**, 882 (2008).
15. A. G. Quiroga, L. Cubo, E. de Blas, P. Aller, C. Navarro-Ranninger, *J. Inorg. Biochem.*, **101**, 104 (2007).
16. H. I. Hall, K. Taylor, M. C. Miller, X. Dothan, M. A. Khan, F. M. Bouet, *Anticancer Res.*, **17**, 2411 (1997).
17. D. Jayaraju, A. K. Kondapi, *Curr. Science*, **81**, 787 (2001).
18. a) N. Saglam, A. Colak, K. Serbest, S. Dülger, S. Güner, S. Karaböcek, A. O. Beldüz, *Biometals*, **15**, 357 (2002); b) K. Serbest, S. Karaböcek, İ. Değirmencioğlu, S. Güner, *Trans. Metal Chem.*, **26**, 375 (2001).
19. M. S. S. Babu, K. H. Reddy, P. G. Krishna, *Polyhedron*, **26**, 572 (2007).
20. S. Anbu, M. Kandaswamy, P. Suthakaran, V. Murugan, B. Varghese, *J. Inorg. Biochem.*, **103**, 401 (2009).
21. R. G. Kurmangalieva, I. A. Poplavskaya, K. A. Abdulin, T. A. Andreyanova, T. S. Safonova, *Pharm. Chem. J.*, **26**, 730 (1992).
22. S. Soga, Y. Shiotsu, S. Akinaga, S. V. Sharma, *Curr. Cancer Drug Targets*, **3**, 359 (2003).
23. J.-G. Cui, L. Fan, L.-L. Huang, H.-L. Liu, A.-M. Zhou, *Steroids*, **74**, 62 (2009).
24. H.-J. Park, K. Lee, S.-J. Park, B. Ahn, J.-C. Lee, H. Y. Cho, K.-I. Lee, *Bioorg. Med. Chem. Lett.*, **15**, 3307 (2005).
25. S. Rajabalian, A. Foroumadi, A. Shafiee, S. Emani, *J. Pharm. Pharmaceut. Sci.*, **10**, 153 (2007).
26. K. Cui, L. Wang, H. Zhu, S. Gou, Y. Liu, *Bioorg. Med. Chem. Lett.*, **16**, 2937 (2006).
27. A. Garoufis, S. K. Hadjikakou, N. Hadjiliadis, *Coord. Chem. Rev.*, **253**, 1384 (2009).
28. H. Wieland, *Ber.*, **43**, 3362 (1910).
29. Oxford Diffraction, *CrysAlis RED*, *CrysAlisCCD (Version 1.171.30) and KM4CCD*, Oxford Diffraction Ltd., Abingdon, Oxfordshire, UK (2004).
30. a) G. M. Sheldrick, *SHELXS97*, *Program for the Solution of Crystal Structures*, University of Göttingen, Germany (1997); b) G. M. Sheldrick, *SHELXL97*, *Program for the Refinement of Crystal Structures*, University of Göttingen, Germany (1997).
31. H. E. Gottlieb, V. Kotlyar, A. Nudelman, *J. Org. Chem.*, **62**, 7512 (1997).
32. R. K. Harris, E. D. Becker, S. M. Cabral de Menezes, P. Granger, R. E. Hoffman, K. W. Zilm, *Pure Appl. Chem.*, **80**, 59 (2008).
33. T. Mosmann, *J. Immunol. Methods*, **65**, 55 (1983).
34. K. Mereiter, Technical University of Vienna, Private communication (2003).
35. J. K. Maurin, *Acta Cryst.*, *C*, **51**, 2111 (1995).
36. a) Yu. A. Simonov, T. Yu. Sliva, M. D. Mazus, A. A. Dvorkin, R. D. Lampeka, *Zh. Neorg. Khim.*, **34**, 873 (1995) [*Chem. Abstr.*, **111**, 89292c (1989)]; b) A. A. Dvorkin, Yu. A. Simonov, T. Yu. Sliva, R. D. Lampeka, M. D. Mazus, V. V. Skopenko, T. I. Malinovskii, *Zh. Neorg. Khim.*, **34**, 2582 (1989) [*Chem. Abstr.*, **112**, 150654m (1990)]; c) V. V. Skopenko, T. Yu. Sliva, Yu. A. Simonov, A. A. Dvorkin, M. D. Mazus, R. D. Lampeka, T. I. Malinovskii, *Zh. Neorg. Khim.*, **35**, 1743 (1990) [*Chem. Abstr.*, **113**, 243530d (1990)]; d) R. D. Lampeka, Z. D. Uzakbergenova, V. V. Skopenko, *Z. Naturforsch.*, *B*, **48**, 409 (1993); e) R. D. Lampeka, N. M. Dudarenko, V. V. Skopenko, *Acta Cryst.*, *C*, **50**, 706 (1994); R. Lampeka, R. Bergs, R. Kramer, K. Polborn, W. Beck, *Z. Naturforsch., B*, **49**, 225 (1994); f) R. Bergs, R. Lampeka, C. Robl, W. Beck, *Z. Naturforsch.*, *B*, **49**, 483 (1994).
37. M. V. Kirillova, M. Haukka, A. M. Kirillov, J. A. L. Silva, J. A. R. Fraústo da Silva, A. J. L. Pombeiro, *Acta Cryst.*, *E*, **63**, m1670 (2007).
38. A. A. Bagabas, A. W. Apblett, A. M. Shemsi, Z. S. Seddigi, *Main Group Chem.*, **7**, 65 (2008).
39. S. J. Berners-Price, L. Ronconi, P. J. Sadler, *Progr. Nucl. Magnet. Reson. Spectrosc.*, **49**, 65 (2006).
40. J. R. L. Priqueler, I. S. Butler, F. D. Rochon, *Appl. Spectrosc. Rev.*, **41**, 185 (2006).
41. R. M. Silverstein, G. C. Bassler, T. C. Morrill, *Spectrometric Identification of Organic Compounds* (Russian), 3rd edn., Mir, Moscow (1977).
42. N. I. Dodoff, D. Kovala-Demertzi, M. Kubiak, J. Kuduk-Jaworska, A. Kochel, G. A. Gorneva, *Z. Naturforsch.*, *B*, **61**, 1110 (2006).
43. a) F. D. Rochon, G. Massarweh, *Inorg. Chim. Acta*, **359**, 4095 (2006); b) F. D. Rochon, C. Bonnier, *Inorg. Chim. Acta*, **360**, 461 (2007); c) F. D. Rochon, C. Tessier, V. Buculei, *Inorg. Chim. Acta*, **360**, 2255 (2007); d) F. Rochon, C. Bensimon, C. Tessier, *Inorg. Chim. Acta*, **361**, 16 (2008); e) F. D. Rochon, P. S. Dieng, *Inorg. Chim. Acta*, **361**, 1222 (2008).
44. G. C. Levy, R. L. Lichter, G. L. Nelson, *Carbon-13 Nuclear Magnetic Resonance Spectroscopy*, 2nd edn., 136–137, 161–162, John Wiley & Sons, New York (1980).
45. E. Breitmaier, *Structure Elucidation by NMR in Organic Chemistry,* 14–15, 27–29, John Wiley & Sons, Chichester (1993).
46. T. D. W. Claridge, *High Resolution NMR Techniques in Organic Chemistry*, 2nd edn., 79–80, Elsevier, Oxford (2009).
47. S. van Zutphen, E. Pantoja, R. Soriano, C. Soro, D. M. Tooke, A. L. Spek, H. den Dulk, J. Brower, J. Reedijk, *J. Chem. Soc. Dalton Trans.*, 1020 (2006).
48. W.-C. Su, S.-L. Chang, T.-Y. Chen, J.-S. Chen, C.-J. Tsao, *Jpn. J. Clin Oncol.*, **30**, 562 (2000).
49. C. M. Riley, L. A. Sternson, in: K. Florey (ed.), *Analytical Profiles of Drug Substances*, Vol. 14, 78–105, Academic Press, New York (1985).
50. K. R. Harrap, *Cancer Treat Rev.*, **12**, Suppl. A, 21 (1985).
51. S. Elmore, *Toxicol. Pathol.*, **35**, 495 (2007).
52. T. Boulikas, M. Vougiouka, *Oncol. Rep.*, **10**, 1663 (2003).